Pergamon

Int. J. Solids Structures Vol. 33, No. 4, pp. 577–594, 1996

0020–7683/96 $9.50 + .00

0020–7683(94)00255–X

DESIGN SENSITIVITY ANALYSIS IN DYNAMIC THERMOVISCOELASTICITY WITH IMPLICIT INTEGRATION

MICHAEL J. POLDNEFF

The Goodyear Tire & Rubber Company, Department 431A-TC, P. O. Box 3531, Akron, OH 44309, U.S.A.

and

JASBIR S. ARORA

Optimal Design Laboratory, Department of Civil Engineering, College of Engineering, The University of Iowa, Iowa City, IA 52242, U.S.A.

(*Received* 17 *March* 1994; *in revised form* 10 *October* 1994)

Abstract—Design sensitivity equations for coupled thermoviscoelastic systems are discretized via the finite element method. The approach is developed for structural systems by using the total Lagrangian approach and the reference domain concept. The discretization is based on implicit integration schemes. The implementation of finite element and design sensitivity analysis utilizes the Christensen–Naghdi free energy function and the direct differentiation approach, which is most suitable for the systems under consideration. A relationship between the discretized sensitivity equations and the equations for the original analysis is shown. Use of the same discretization for analysis and sensitivity analysis is emphasized. Partial derivatives of the right-hand side required for sensitivity calculations are implemented via the central difference method, which provides greater flexibility without sacrificing accuracy. Examples of analysis and design sensitivity analysis for a thermoviscoelastic non-linear truss and a plate with a hole are given. The calculated sensitivity results are verified by comparison with overall finite difference calculations.

1. INTRODUCTION

Finite element (FE) analysis in engineering applications has advanced recently and includes such an important area for engineering applications as analysis of thermoviscoelastic structures. Examples of such structural systems may be systems composed of polymeric materials, whose hysteretic and viscoelastic properties necessitate coupled thermo-viscoelastic analysis to capture some important aspects of their behavior. Since, typically, engineering analysis is geared toward design improvement (or optimization), design sensitivity analysis (DSA) of such structures should be performed to expedite this process.

A number of papers have been published recently on DSA of thermoelastic and thermoviscoplastic structures by Meric (1986a,b, 1987, 1988, 1990), Dems (1987), Dems and Mroz (1987), Hou *et al.* (1990), Tortorelli *et al.* (1991a,b), and Lee *et al.* (1991, 1993). An approach for DSA of thermoviscoelastic structural systems was also recently developed by Poldneff and Arora (1993). In the present study, we discretize the equations that were developed by Poldneff and Arora (1993) via the FE method and implement the approach by using a specific thermoviscoelastic material model described by the free energy function proposed by Christensen and Naghdi (1967). For this particular material model, a computer code for thermoviscoelastic FE analysis DSA, which is based on a direct differentiation method and implicit integration procedures, is developed. Numerical examples demonstrate the development.

Numerical integration procedures that are used in dynamic analysis are generally subdivided into two large groups: explicit and implicit. Procedurally, the major difference is that it is not necessary to solve a system of non-linear algebraic equations for explicit methods in order to calculate primary quantities such as displacements or temperatures

and to advance to the next time step, whereas a system of non-linear algebraic equations has to be solved in the case of implicit methods to obtain the primary quantities and to go to the next time step. Such a system of non-linear equations is usually solved by the iterative Newton–Raphson method. This difference in the procedure for implicit and explicit methods dictates a difference in DSA. Since no equations are solved in the explicit time integration schemes, no advantage is gained, as far as the CPU time is concerned, by the development and implementation of special procedures for DSA: overall finite difference is just as fast. Such a development and implementation, however, may be desirable from the convenience standpoint. On the other hand, in the case of the implicit integration, it is definitely advantageous to develop and implement a DSA procedure that is tied closely to the analysis. In this case, DSA is very economical, since typically only one backsubstitution using the current tangent stiffness matrix (from the Newton–Raphson method for analysis) is required for sensitivity calculations once convergence is achieved. With some constitutive models, it is more appropriate and efficient to use an iterative procedure to solve the sensitivity equation even though it is linear (Jao and Arora, 1992). In the current development, we focus on DSA that is based on an FE analysis with an implicit integration.

2. FIELD EQUATIONS

As in our previous work (Poldneff and Arora, 1993), we consider a solid deformable body subjected to external forces and heat sources. The system of equations describing its behavior consists of equations for balance of momentum, conservation of energy, constitutive functionals, and compatibility, together with appropriate boundary and initial conditions, which we consider in the undeformed configuration. We discretize the equations by using FEM and later examine their relation to the DSA equations.

We first write the momentum and energy equations in a weak form and then subdivide the domain occupied by the system into FE. We approximate spatial co-ordinates, displacements, and temperature by using the the shape functions N_A, which are defined in the standard element according to the isoparametric FE concept. Subscript A refers to the element node in the sense that N_A has unit value at the node A and zero at the rest of the element nodes. We then obtain the discretized versions of the equations of motion and energy:

$$m_{AB}\ddot{u}_i^B + \int_D J z_{ij} d_{sj} \sigma_{kl} d_{lk} N_{B,l} \, \mathrm{d}D = G_{Bi} \tag{1}$$

$$\left(\int_D J\rho N_A \dot{\eta} N_B \, \mathrm{d}D\right) T^A - \int_D J q_l d_{kl} N_{B,k} \, \mathrm{d}D = \int_{\Gamma_q} J_\Gamma \bar{q} N_B \, \mathrm{d}\Gamma_q - \int_{\Gamma_c} J_\Gamma h (T_I^A - T^A) N_A N_B \, \mathrm{d}\Gamma + \int_{\Gamma_R} J_\Gamma R[(N_A T_R^A)^4 - (N_A T^A)^4] N_B \, \mathrm{d}\Gamma + \int_D J\rho r N_B \, \mathrm{d}D + \int_D J\omega N_B \, \mathrm{d}D \tag{2}$$

where the mass matrix m_{AB} and the right-hand side G_{Bi} are given by the following expressions:

$$m_{AB} = \int_D \rho N_A N_B J \, \mathrm{d}D$$

$$G_{Bi} = \int_\Gamma J_\Gamma \bar{S}_i N_B \, \mathrm{d}\Gamma + \int_D J\rho F_i N_B \, \mathrm{d}D$$

A semicolon in all the above equations denotes partial differentiation with respect to the co-ordinates in the reference configuration. The quantities used in eqns (1) and (2) are as follows: u_i are the components of displacement, J is the Jacobian determinant of the transformation from the reference to the undeformed configuration, z_1, z_2, z_3 are the co-ordinates of a point in the deformed configuration, d_{kl} are the elements of the J^{-1} matrix, σ_{ij} are the components of the second Piola–Kirchoff stress tensor, D is the reference domain, ρ is the mass density in the undeformed configuration, η is the specific entropy, q_i are the components of heat flux, J_Γ is the Jacobian determinant of the mapping of the boundary in the reference domain onto the boundary in the undeformed configuration, $\bar{q}$ is the prescribed heat flux, h is the convective coefficient, T is the absolute temperature, T_f is the fluid temperature, R is the radiation coefficient, T_R is the temperature of the radiative source, r is the heat supply per unit mass, $\bar{S}_i$ are the components of surface traction, F_i are the components of body force, and ω is the internal dissipation; it is used as by Poldneff and Arora (1993). We note that integrals in eqns (1) and (2) are over the reference domain or its boundary. For the isoparametric elements, the reference domain is the standard element that is mapped into a real element. It is therefore clear that the reference volume approach is very well suited to FE implementation.

To complete the discretization, we consider the constitutive equations in the discretized form. The constitutive functionals are written as follows:

$$\sigma_{ij} = \overset{t}{\underset{\tau=0}{\Xi_{ij}}}(\varepsilon_{st}, T) \tag{3}$$

$$\eta = \overset{t}{\underset{\tau=0}{\Theta}}(\varepsilon_{st}, T) \tag{4}$$

$$q_i = \overset{t}{\underset{\tau=0}{Q_i}}(u_{l,m}, \varepsilon_{st}, T, g_k) \tag{5}$$

$$\omega = \overset{t}{\underset{\tau=0}{\Omega}}(\varepsilon_{st}, T) \tag{6}$$

where a comma denotes partial differentiation with respect to the co-ordinates in the undeformed configuration, ε_{ij} are the components of the Green–Lagrange strain tensor, and g_k are the temperature gradients.

We next subdivide the time interval into a collection of subintervals of duration Δt_n and define discrete moments in time t_n, $t_n = t_{n-1} + \Delta t_n$ with $t_0 = 0$. Since eqns (3)–(6) depend on the whole history of the variables, at the time moment t_n, the dependence will be on the variables at all the time moments prior to and including t_n, that is we can rewrite the discrete equivalent of the constitutive equations as:

$$\sigma_{kl}^n = \sigma_{kl}^n(\varepsilon_{st}^0, \varepsilon_{st}^1, \ldots, \varepsilon_{st}^n, T^0, T^1, \ldots, T^n) \tag{7}$$

$$\eta = \eta^n(\varepsilon_{st}^0, \varepsilon_{st}^1, \ldots, \varepsilon_{st}^n, T^0, T^1, \ldots, T^n) \tag{8}$$

$$q_i^n = q_i^n(u_{l,m}^n, \varepsilon_{st}^0, \varepsilon_{st}^1, \ldots, \varepsilon_{st}^n, T^0, T^1, \ldots, T^n, g_k^0, g_k^1, \ldots, g_k^n) \tag{9}$$

$$\omega^n = \omega^n(\varepsilon_{st}^0, \varepsilon_{st}^1, \ldots, \varepsilon_{st}^n, T^0, T^1, \ldots, T^n) \tag{10}$$

superscript in the above equations specifies the point in time.

By using specific constitutive laws and numerical schemes for time discretization, eqns (7)–(10) are readily obtained from eqns (3)–(6). In order to write algebraic equations amenable to computer implementation, we shall perform temporal discretization with the Newmark scheme for displacements and the Crank–Nicholson scheme for temperatures. All the following conclusions, however, remain valid for any implicit temporal discretization.

Applying the temporal discretization to the weak form of the equations of motion and energy, we obtain:

$$m_{AB}\left[\frac{u_i^{An+1}}{\beta(\Delta t)^2}-\frac{u_i^{An}}{\beta(\Delta t)^2}-\frac{\dot{u}_i^{An}}{\beta\Delta t}-\frac{(1-2\beta)\ddot{u}_i^{An}}{2\beta}\right]+\int_D J z_{iS}^{n+1} d_{sj}\sigma_{kj}^{n+1}\,\mathrm{d}_{lk}N_{B;l}\mathrm{d}D=G_{Bi}^{n+1} \tag{11}$$

$$\begin{aligned}
&P_{AB}(\varepsilon_{ST}^0,\varepsilon_{ST}^1,\ldots,\varepsilon_{ST}^{n+1},T^0,T^1,\ldots,T^{n+1})T^{An+1}\\
&\quad-\int_D Jq_i(u_{i;m}^{n+1},\varepsilon_{ST}^0,\varepsilon_{ST}^1,\ldots,\varepsilon_{ST}^{n+1},T^0,T^1,\ldots,T^{n+1},g_k^0,g_k^1,\ldots,g_k^{n+1})d_{ki}N_{B;k}dD\\
&=\int_{\Gamma_q} J_\Gamma \bar{q}^{n+1}N_B d\Gamma_q+\int_{\Gamma_h} J_\Gamma h(T_f^{An+1}-T^{An+1})N_A N_B\,\mathrm{d}\Gamma\\
&\quad+\int_{\Gamma_R} J_\Gamma R[(N_A T_R^{An+1})^4-(N_A T^{An+1})^4]N_B\,\mathrm{d}\Gamma+\int_D J\rho r^{n+1}N_B\,\mathrm{d}D\\
&\quad+\int_D J\omega(\varepsilon_{ST}^0,\varepsilon_{ST}^1,\ldots,\varepsilon_{ST}^n,T^0,T^1,\ldots,T^n)N_B\,\mathrm{d}D
\end{aligned} \tag{12}$$

where P_{AB} is related to the constitutive equation for entropy.

Equations (11) and (12) are non-linear algebraic equations with respect to the current values of displacements and temperatures, but they depend on all the past values of displacements and temperature. In order to start the process, we use the initial values of displacements, velocities, and temperatures. The initial values for accelerations and temperature rates are calculated by using the prescribed initial conditions in eqns (11) and (12). The solution of the derived equations is obtained iteratively by using the Newton–Raphson method, which is widely used for the solution of systems of simultaneous non-linear equations and is a popular tool in the non-linear FE technology. We take partial derivatives of equations with respect to the unknowns to find the expressions for the tangent stiffness matrix for the Newton–Raphson method. Differentiating eqns (11) and (12) with respect to the nodal unknown displacements u_α^{Cn+1} and temperatures T^{Dn+1}, we obtain:

$$\begin{aligned}
&\frac{m_{AB}\delta_{i\alpha}}{(\beta\Delta t)^2}+\int_D Jz_{iS}^{n+1}d_{sj}\frac{\partial\sigma_{kj}^{n+1}}{\partial\varepsilon_{rp}^{n+1}}\frac{\partial\varepsilon_{rp}^{n+1}}{\partial u_\alpha^{Cn+1}}d_{lk}N_{B;l}\,\mathrm{d}D\\
&\qquad-\int_D Jd_{sj}\sigma_{kj}^{n+1}d_{lk}N_{B;l}\,\mathrm{d}D-\frac{\partial G_{Bi}^{n+1}}{\partial u_\alpha^{Cn+1}}=E_{BiC\alpha}^u
\end{aligned} \tag{13}$$

$$\int_D Jz_{iS}^{n+1}d_{sj}\frac{\partial\sigma_{kj}^{n+1}}{\partial T^{Dn+1}}d_{lk}N_{B;l}\,\mathrm{d}D=E_{BiD}^T \tag{14}$$

$$\begin{aligned}
&\frac{\partial(P_{AB}T^{An+1})}{\partial u_\alpha^{Cn+1}}-\int_D J\left(\frac{\partial q_i}{\partial u_{j;m}}d_{sm}N_{C;s}+\frac{\partial q_i}{\partial\varepsilon_{rp}^{n+1}}\frac{\partial\varepsilon_{rp}^{n+1}}{\partial u_\alpha^{Cn+1}}\right)d_{lk}N_{B;l}\,\mathrm{d}D\\
&\qquad-\int_D J\frac{\partial\omega}{\partial\varepsilon_{rp}^{n+1}}\frac{\partial\varepsilon_{rp}^{n+1}}{\partial u_\alpha^{Cn+1}}N_B\,\mathrm{d}D-\frac{\partial Q_B}{\partial u_\alpha^{Cn+1}}=L_{BC\alpha}^u
\end{aligned} \tag{15}$$

$$\frac{\partial(P_{AB}T^{An+1})}{\partial T^{Dn+1}} - \int_D J\left(\frac{\partial q_i}{\partial T^{n+1}} N_D + \frac{\partial q_i}{\partial q_k^{n+1}} N_{D,k} d_{ik}\right) d_{jl} N_{B,l}\, \mathrm{d}D + \int_D J \frac{\partial \omega}{\partial T^{n+1}} N_B N_D\, \mathrm{d}D$$

$$- \int_{\Gamma_h} J_1 h N_B N_D\, \mathrm{d}\Gamma + \int_{\Gamma_R} J_1 R 4 N_D^4 (T^{Dn+1})^3 N_B\, \mathrm{d}\Gamma = L_{BD}^T \quad (16)$$

Quantities $E_{BiC\alpha}^u$, E_{BiD}^T, $L_{BC\alpha}^u$, and L_{BD}^I are parts of the tangent stiffness matrix; B, C, and D are node numbers; i and α are degrees of freedom; and superscripts u and T denote the variable used in the partial differentiation: either displacement or temperature. It is clear that $E_{BiC\alpha}^u$ is responsible for the mechanical part, L_{BD}^T is responsible for the thermal part, and E_{BiD}^T and $L_{BC\alpha}^u$ are responsible for the coupling between the mechanical and thermal parts.

The tangent stiffness matrix $\mathbf{K}$ is used in the Newton–Raphson iterations to solve the following systems of linear simultaneous equations:

$$\mathbf{K}\Delta s_{n+1}^j = R^j \quad (17)$$

where j is the iteration number, s is the unknown vector combining nodal displacements and temperatures, and $\mathbf{R}^j$ is the residual.

When eqns (17) are solved, the solution vector s_{n+1}^j is updated $s_{n+1}^{j+1} = s_{n+1}^j + \Delta s_{n+1}^j$, and the residual is checked against the specified tolerance. If the tolerance is not met, iterations go on. If the tolerance is met, time is incremented, and iterations begin at the next point in time.

3. DIRECT DIFFERENTIATION METHOD

To discretize the DDM equations obtained by Poldneff and Arora (1993), we follow the same FE procedure as in the previous section. Then, using the same finite element shape functions, we obtain discretized sensitivity equations analogous to the discretized equations of motion and energy:

$$m_{AB}\delta\ddot{u}_i^A + \left[\int_D J N_{A,s} d_{sl}\sigma_{kl} d_{jk} N_{B,l}\, \mathrm{d}D\right]\delta u_i + \int_D J z_{ts} d_{sl} \hat{K}^{kl}_{\Xi\varepsilon_{mn}}(\delta\varepsilon_{mn}) N_{B,l} d_{jk}\, \mathrm{d}D$$

$$+ \int_D J z_{ts} d_{sj} \hat{K}^{kj}_{\Xi T}(\delta T) N_{B,l} d_{jk}\, \mathrm{d}D = H_{Bi}$$

$$\left(\int_D \rho J N_A \dot{\eta} N_B\, \mathrm{d}D\right)\delta T^A + \int_D \rho J T \hat{K}'_{\Theta\varepsilon_{ij}}(\delta\varepsilon_{ij}) N_B\, \mathrm{d}D + \int_D \rho J T \hat{K}'_{\Theta T}(\delta T) N_B\, \mathrm{d}D$$

$$- \int_D J\left[D_{w_{ip}} \int_0^t \dot{Q}_i' \delta w_{ip} + \hat{K}'_{Q\varepsilon_{lm}}(\delta\varepsilon_{lm}) + \hat{K}'_{Qq_m}(\delta q_m) + \hat{K}'_{QT}(\delta T)\right] \mathrm{d}_{ki} N_{B,k}\, \mathrm{d}D$$

$$- \int_D J(\delta\sigma_{lm}\dot{\varepsilon}_{lm} + \sigma_{lm}\delta\dot{\varepsilon}_{lm} - \rho[\hat{K}_{\Psi\varepsilon_{ij}}(\delta\varepsilon_{ij}) + \hat{K}_{\Psi T}(\delta T) + (\hat{K}_{\Theta\varepsilon_{ij}}(\delta\varepsilon_{ij})$$

$$+ \hat{K}_{\Theta T}(\delta T))\dot{T} + \eta\delta\dot{T}^A N_A])N_B\, \mathrm{d}D = R_B$$

where δ denotes design variation and

$$H_{Bi} = \delta G_{Bi} - \delta m_{AB}\ddot{u}_i^A - \int_D \delta_b(J z_{ts} d_{sj}\sigma_{kl} d_{jk}) N_{B,l}\, \mathrm{d}D$$

with δ_b being partial variation with respect to the design parameter b. Linear hereditary functionals $\hat{K}^{kj}_{\Xi\varepsilon_{mn}}$, $\hat{K}^{kj}_{\Xi T}$, etc., are defined by Poldneff and Arora (1993) and are obtained by

taking Frechet differentials of the non-linear constitutive functionals. In this particular notation, the first subscript denotes the constitutive functional that is differentiated, the second superscript denotes the variable in Frechet differentiation; superscripts represent the functional that is differentiated; a prime means that the functional is differentiated with respect to time.

Applying the same time discretization as in the previous section, i.e. Newmark and Crank–Nicholson schemes, we arrive at the following discretized equations for sensitivities in DDM:

$$m_{AB}\left[\frac{\delta u_i^{An+1}}{\beta(\Delta t)^2}-\frac{\delta u_i^{An}}{\beta(\Delta t)^2}-\frac{\delta \dot{u}_i^{An}}{\beta\Delta t}-\frac{(1-2\beta)\delta\ddot{u}_i^{An}}{2\beta}\right]+\left(\int_D Jd_{sj}\sigma_{kj}^{n+1}d_{lk}N_{B,l}\,\mathrm{d}D\right)\delta u_i^{An+1}$$
$$+\int_D Jz_{i,s}^{n+1}d_{sj}\frac{\partial\sigma_{kj}^{n+1}}{\partial\varepsilon_{rp}^{\beta}}\frac{\partial\varepsilon_{rp}^{\beta}}{\partial u_\gamma^{C\beta}}d_{lk}N_{B,l}\,\mathrm{d}D+\int_D Jz_{i,s}^{n+1}d_{sj}\frac{\partial\sigma_{kj}^{\beta}}{\partial T^{D\beta}}d_{lk}N_{B,l}\,\mathrm{d}D-\frac{\partial G_{Bi}^{n+1}}{\partial u_\chi^{Cn+1}}$$
$$=-\delta m_{AB}\left[\frac{u_i^{An+1}}{\beta(\Delta t)^2}-\frac{u_i^{An}}{\beta(\Delta t)^2}-\frac{\dot{u}_i^{An}}{\beta\Delta t}-\frac{(1-2\beta)\ddot{u}_i^{An}}{2\beta}\right]+\delta_b G_{Bi}-\int_D\delta_b(Jz_{i,s}d_{sj}\sigma_{kj}d_{lk})N_{B,l}\,\mathrm{d}D \quad (18)$$

$$\frac{\partial(P_{AB}T^{An+1})}{\partial u_\chi^{C\beta}}\delta u_\chi^{C\beta}+\frac{\partial(P_{AB}T^{An+1})}{\partial T^{D\beta}}\delta T^{D\beta}+\frac{\partial(P_{AB}T^{An+1})}{\partial b}\delta b$$
$$-\left[\int_D J\left(\frac{\partial q_i}{\partial u_{j,m}}d_{sm}N_{C,s}+\frac{\partial q_i}{\partial\varepsilon_{rp}^{\beta}}\frac{\partial\varepsilon_{rp}^{\beta}}{\partial u_\gamma^{C\beta}}\right)d_{lk}N_{B,l}\,\mathrm{d}D\right]\delta u_\chi^{C\beta}$$
$$-\left[\int_D J\left(\frac{\partial q_i}{\partial T^{\beta}}N_D+\frac{\partial q_i}{\partial q_k^{\beta}}N_{D,s}d_{sk}\right)d_{li}N_{B,l}\,\mathrm{d}D\right]\delta T^{\beta}$$
$$-\left[\int_D J\frac{\partial q_i}{\partial b}d_{li}N_{B,l}\,\mathrm{d}D\right]\delta b-\left[\int_D J\frac{\partial\omega}{\partial\varepsilon_{rp}^{\beta}}\frac{\partial\varepsilon_{rp}^{\beta}}{\partial u_\chi^{C\beta}}N_B\,\mathrm{d}D\right]\delta u_\chi^{C\beta}$$
$$-\left[\int_D J\frac{\partial\omega}{\partial T^{D\beta}}N_BN_D\,\mathrm{d}D\right]\delta T^{D\beta}-\left[\int_D J\frac{\partial\omega}{\partial b}N_B\,\mathrm{d}D\right]\delta b$$
$$+\left[\int_{\Gamma_h}J_\Gamma hN_BN_D\,\mathrm{d}\Gamma\right]\delta T^{An+1}+\left[\int_{\Gamma_R}J_\Gamma R4N_D^4(T^{Dn+1})^3N_B\,\mathrm{d}\Gamma\right]\delta T^{An+1}$$
$$=-\int_D\delta(J\rho)N_A\dot{\eta}T^4N_B\,\mathrm{d}D+\int_D\delta J\omega N_B\,\mathrm{d}D$$
$$+\delta\int_{\Gamma_q}J_\Gamma\bar{q}N_B\,\mathrm{d}\Gamma_q+\int_{\Gamma_h}J_\Gamma hT_f^4N_AN_B\,\mathrm{d}\Gamma+\int_{\Gamma_R}J_\Gamma R(N_AT_R^4)^4N_B\,\mathrm{d}\Gamma$$
$$+\int_D J\rho rN_B\,\mathrm{d}D)+\int_D q_i\delta(Jd_{kl})N_{B,k}\,\mathrm{d}D \quad (19)$$

The superscript β in eqns (18) and (19) has a range of values from 0 to n+1, which thus accounts for the history of deformations.

Comparing eqns (18) and (19) with eqns (13)–(16), we can conclude that, for solution of the sensitivity problem by using DDM, a system of linear equations that has the following structure has to be solved:

(i) the matrix of the system coincides with the tangent stiffness matrix of the analysis problem for the same time step as when the solution has converged;
(ii) the right-hand side F of the sensitivity system is related to the residual vector **R** of the analysis problem with a converged solution in the following manner:

$$\mathbf{F} = \frac{\partial \mathbf{R}}{\partial b}\delta b + \frac{\partial \mathbf{R}}{\partial u_z^{Da}}\delta u_z^{Da} + \frac{\partial \mathbf{R}}{\partial T^{Da}}\delta T^{Da}. \tag{20}$$

Superscript a in eqn (20) takes values from 0 to n, so the summation for this superscript is over the past history excluding the current time t_{n+1}.

We note that both **R** and **F** have to be generally recalculated from one time increment to the next. However, for some particular cases (linear thermoviscoelasticity, for example), they can be calculated just by adding extra terms to the values from the previous time step.

The DDM can be implemented along with the response analysis: as soon as the analysis problem has converged at a certain time step, the right-hand side for the sensitivity problem can be formed, and the sensitivity analysis solution can be obtained by making use of the current tangent stiffness matrix. The solution process can then march on in time along with the sensitivity analysis. Since the sensitivity results are correct only for the exact solution of the non-linear algebraic equations, the tolerance on the convergence has to be fairly tight for good accuracy. It may be seen that the right-hand side of the sensitivity equations is obtained by partial differentiation of the residual vector with respect to the design parameter, b, and by carrying along the past history sensitivities. The sensitivities therefore depend not only on the history of displacements and temperature but also on the history of displacement and temperature sensitivities.

4. IMPLEMENTATION

4.1 *Constitutive Equations*

We consider constitutive equations proposed by Christensen and Naghdi (1967). They were discussed in detail by Poldneff and Arora (1993). For isotropic materials, the equations for stresses and entropy take the form:

$$\sigma_{ij} = \int_0^t 2G(t-\tau)\frac{\partial \varepsilon_{ij}(\tau)}{\partial \tau}\,\mathrm{d}\tau + \tfrac{1}{3}\delta_{ij}\int_0^t \lambda(t-\tau)\frac{\partial \varepsilon_{kk}(\tau)}{\partial \tau}\,\mathrm{d}\tau - \alpha\delta_{ij}\int_0^t 3K(t-\tau)\frac{\partial T(\tau)}{\partial \tau}\,\mathrm{d}\tau \tag{21}$$

$$\rho S = \alpha\int_0^t 3K(t-\tau)\frac{\partial \varepsilon_{kk}(\tau)}{\partial \tau}\,\mathrm{d}\tau + \rho\int_0^t m(t-\tau)\frac{\partial T(\tau)}{\partial \tau}\,\mathrm{d}\tau \tag{22}$$

where G, λ, and K are kernels similar to the Lame constants and bulk modulus in elasticity; α is the coefficient of thermal expansion; m is a kernel similar to the specific heat quantity in heat transfer; ρ is the mass density; ε_{ij} are the strain components; and T denotes temperature change with respect to initial temperature T_0.

For computer implementation, we assume that every kernel Γ in eqns (21) and (22) can be represented by a sum of exponents with a certain amplitude A_i^Γ and relaxation time v_i^Γ, that is:

$$\Gamma(t) = A_0^\Gamma + \sum_{i=1}^{N} A_i^\Gamma \exp\left(-\frac{t}{v_i^\Gamma}\right) \tag{23}$$

where superscript Γ denotes the kernel for which a constant is used.

As was shown by Poldneff and Arora (1993), in order to satisfy the Second Law, the constitutive equations relating the heat flux and the temperature gradients have to be taken in the classical Fourier law form:

$$q_i = -\kappa_{ij}T_{,j} \tag{24}$$

where κ_{ij} are thermal conductivities.

4.2 *Specific discretization*

To arrive at the special form of FE equations, first consider infinitesimal displacements u_k; that is the strain–displacement relations assume the form

$$\varepsilon_{ij} = \tfrac{1}{2}(u_{i,j} + u_{j,i}).$$

We substitute the strain–displacement relations and constitutive eqns (21), (22) and (24) into a weak form of momentum and entropy eqns (1), (2). Performing the required operations, we obtain, similarly to Oden (1972), the following discretized differential equations of motion and energy:

$$m_{AB}\ddot{u}_i^A + a_{BiAk}\int_0^t G(t-\tau)\dot{u}_k^A(\tau)\,\mathrm{d}\tau + b_{BiAk}\int_0^t \lambda(t-\tau)\dot{u}_k^A(\tau)\,\mathrm{d}\tau + c_{BiA}\int_0^t K(t-\tau)\dot{T}^A(\tau)\,\mathrm{d}\tau = G_{Bi} \quad (25)$$

$$d_{BAk}\dot{u}_k^A + f_{BAk}\int_0^t \frac{\partial K(t-\tau)}{\partial t}\dot{u}_k^A(\tau)\,\mathrm{d}\tau + g_{BA}\dot{T}^A + h_{BA}\int_0^t \frac{\partial m(t-\tau)}{\partial t}\dot{T}^A(\tau)\,\mathrm{d}\tau + \kappa_{BA}T^A = E_B \quad (26)$$

where E_B is the right hand side of eqn (2), and matrices a_{BiAk}, b_{BiAk}, c_{BiA}, d_{BAk}, f_{BAk}, g_{BA}, and g_{BA} are expressed in terms of shape functions as follows:

$$a_{BiAk} = \int_D JN_{B,l}d_{li}(\delta_{ik}N_{A,s} + \delta_{ik}N_{A,s}d_{sj})\,\mathrm{d}D$$

$$b_{BiAk} = \int_D JN_{B,l}d_{li}N_{A,s}d_{sk}\,\mathrm{d}D$$

$$c_{BiA} = \int_D JN_{B,l}d_{li}N_A\,\mathrm{d}D$$

$$d_{BAk} = 3\alpha K_0 T_0 \int_D JN_{A,s}d_{sk}N_B\,\mathrm{d}D$$

$$f_{BAk} = m_0 T_0 \int_D \rho JN_A N_B\,\mathrm{d}D$$

$$h_{BA} = T_0 \int_D \rho JN_A N_B\,\mathrm{d}D$$

$$\kappa_{BA} = \int_D JK_{ij}N_{A,s}d_{sj}N_{B,l}d_{li}\,\mathrm{d}D.$$

We also consider plane trusses undergoing infinitesimal strains, but which could experience finite displacements. Considering the infinitesimal strain condition and the fact that there is only one stress component that is normal to the cross-section and constant along the truss element axis, the equations take the form:

$$m_{AB}\ddot{u}_1^A + (-1)^B\sigma\cos\Phi = G_{B1}$$

$$m_{AB}\ddot{u}_2^A + (-1)^B\sigma\sin\Phi = G_{B2}$$

$$3\alpha LFT_0\left(K_0\dot{\varepsilon} + \int_0^t \frac{\partial K(t-\tau)}{\partial t}\dot{\varepsilon}(\tau)d\tau\right) + g_{BA}\dot{T}^A + h_{BA}\int_0^t \frac{\partial m(t-\tau)}{\partial t}\dot{T}^A(\tau)d\tau + \kappa_{BA}T^A = E_B \quad (27)$$

where σ is the normal stress in the truss element and Φ is the angle of the truss element with respect to the x_1-axis in the deformed configurations, which is calculated in terms of nodal co-ordinates and displacements as follows:

$$\cos\Phi = \frac{x_1 + u_1}{L}$$

$$\sin\Phi = \frac{x_2 + u_2}{L}$$

where L is the element length, F is the element cross-sectional area, and ε is the element strain expressed in terms of nodal displacements as follows:

$$\varepsilon = \frac{u_1^2 - u_1^1}{L}\cos\phi + \frac{u_2^2 - u_2^1}{L}\sin\phi + \frac{1}{2}\left[\left(\frac{u_1^2 - u_1^1}{L}\right)^2 + \left(\frac{u_1^2 - u_1^1}{L}\right)^2\right] \tag{28}$$

ϕ being the truss element angle with respect to the x_1-axis in the undeformed configuration. Despite the linearity of the constitutive equations, eqns (27) and (28) constitute a system of non-linear equations because the strain–displacement relations, eqn (28), are non-linear and the motion equations are written in the deformed configurations.

4.3 *Time integration*

For temporal discretization of the mechanical part, we use the Newmark method (unconditionally stable for linear mechanical systems):

$$\dot{u}^{n+1} = \frac{2}{\Delta t}(u^{n+1} - u^n) - \dot{u}^n$$

$$\ddot{u}^{n+1} = \frac{4}{\Delta t^2}(u^{n+1} - u^n) - \frac{4}{\Delta t}\dot{u}^n - \ddot{u}^n$$

Expressing displacements and velocities in terms of accelerations, we obtain:

$$u^{n+1} = u^n + \Delta t\dot{u}^n + \frac{\Delta t^2}{4}(\ddot{u}^n + \ddot{u}^{n+1}) \tag{29}$$

$$\dot{u}^{n+1} = \dot{u}^n + \frac{\Delta t}{2}(\ddot{u}^n + \ddot{u}^{n+1}). \tag{30}$$

It may be seen from eqns (29) and (30) that in every time interval (t_n, t_{n+1}) displacements are approximated quadratically, and velocities are approximated linearly in time. Keeping this in mind, we discretize a typical integral of velocities in eqns (25) and (26). We subdivide the time interval $(0, t)$ into subintervals, which we use in Newmark approximations, and use the representation of eqn (23) for the kernel. A typical hereditary integral then becomes:

$$\int_0^t \Gamma(t-\tau)\dot{u}(\tau)\,\mathrm{d}\tau = A_0^\Gamma[u(t_{n+1}) - u(0)] + \sum_{i=1}^{N} A_i^\Gamma \exp\left(-\frac{t_{n+1}}{v_i^\Gamma}\right)\sum_{k=0}^{n}\int_{t_k}^{t_{k+1}} \exp\left(\frac{\tau}{v_i^\Gamma}\right)\dot{u}(\tau)\,\mathrm{d}\tau.$$

Approximating $\dot{u}$ linearly in every time interval (t_k, t_{k+1}) and performing closed-form integration, we obtain:

$$\int_0^t \Gamma(t-\tau)\dot{u}(\tau)\,d\tau = A_0^\Gamma(u^{n+1}-u^0) + \sum_{i=1}^{N} A_i^\Gamma \exp\left(-\frac{t_{n+1}}{v_i^\Gamma}\right)\sum_{k=0}^{n}(D_k^{\Gamma i}\dot{u}^k + F_k^{\Gamma i}u^k + G_k^{\Gamma i}u^{k+1}) \quad (31)$$

where $D_k^{\Gamma i}$, $F_k^{\Gamma i}$, $G_k^{\Gamma i}$ are obtained through calculations of integrals such as

$$\int_{t_k}^{t_{k+1}} \exp\left(\frac{\tau}{v_i^\Gamma}\right)d\tau \quad \text{and} \quad \int_{t_k}^{t_{k+1}} \exp\left(\frac{\tau}{v_i^\Gamma}\right)\tau\,d\tau$$

and given by the following expressions:

$$D_k^{\Gamma i} = v_i^\Gamma \exp\left(\frac{t_k}{v_i^\Gamma}\right)\left[\exp\left(\frac{\Delta t}{v_i^\Gamma}\right)-1\right] - \frac{2}{\Delta t}v_i^\Gamma \exp\left(\frac{t_k}{v_i^\Gamma}\right)\left[-v_i^\Gamma\left(\exp\left(\frac{\Delta t}{v_i^\Gamma}\right)-1\right)+\Delta t\exp\left(\frac{\Delta t}{v_i^\Gamma}\right)\right]$$

$$F_k^{\Gamma i} = -\frac{2}{\Delta t^2}v_i^\Gamma \exp\left(\frac{t_k}{v_i^\Gamma}\right)\left[-v_i^\Gamma\left(\exp\left(\frac{\Delta t}{v_i^\Gamma}\right)-1\right)+\Delta t\exp\left(\frac{\Delta t}{v_i^\Gamma}\right)\right]$$

$$G_k^{\Gamma i} = \frac{2}{\Delta t^2}v_i^\Gamma \exp\left(\frac{t_k}{v_i^\Gamma}\right)\left[-v_i^\Gamma\left(\exp\left(\frac{\Delta t}{v_i^\Gamma}\right)-1\right)+\Delta t\exp\left(\frac{\Delta t}{v_i^\Gamma}\right)\right]$$

Two terms, $A_0^\Gamma u_{n+1}$ and

$$\sum_{i=1}^{N} A_i^\Gamma \exp\left(-\frac{t_{n+1}}{v_i^\Gamma}\right)G_n^\Gamma u_{n+1},$$

in eqn (31) contribute to the current stiffness matrix, whereas all others contribute to the right-hand side. We note that the right-hand side for the current time step is calculated by adding terms to the right-hand side of the previous time increment, which thus results in more efficient computations and storage.

The same time integration procedure was used for non-linear truss elements. In that case, Newton–Raphson iterations were used at every time step because of non-linearity. However, because the constitutive law is still linear, that is additive, the same kind of procedure is used for the right-hand side accumulation.

For time integration of the thermal part, we use the Crank–Nicholson method, which provides unconditional stability for thermal problems:

$$\dot{T}^{n+1} = \frac{2}{\Delta t}(T^{n+1}-T^n) - \dot{T}^n$$

Expressing temperatures in terms of temperature rates, we obtain:

$$T^{n+1} = T^n + \frac{\Delta t}{2}(\dot{T}^n + \dot{T}^{n+1}). \quad (32)$$

We can infer from eqn (32) that temperature is approximated linearly in every time interval (t_n, t_{n+1}). Considering this for calculations of typical hereditary integrals of temperature, we obtain:

$$\int_0^t \Gamma(t-\tau)\dot{T}(\tau)\,\mathrm{d}\tau = A_0^\Gamma(T^{n+1}-T^0)+\sum_{i=1}^{N} A_i^\Gamma \exp\left(-\frac{t_{n+1}}{v_i^\Gamma}\right)\sum_{k=0}^{n} H_k^{\Gamma i}(T^{k+1}-T^k)$$

where $H_k^{\Gamma i}$ is obtained through calculations of integrals such as

$$\int_{t_k}^{t_{k+1}} \exp\left(\frac{\tau}{v_i^\Gamma}\right)\mathrm{d}\tau$$

and is calculated as follows:

$$H_k^{\Gamma i} = \frac{v_i^\Gamma}{\Delta t}\exp\left(\frac{t_k}{v_i^\Gamma}\right)\left[\exp\left(\frac{\Delta t}{v_i^\Gamma}\right)-1\right].$$

Again, as in the previous section, a conclusion can be drawn that only terms $A_0^\Gamma T^{n+1}$, and

$$\sum_{i=1}^{N} A_i^\Gamma \exp\left(-\frac{t_{n+1}}{v_i^\Gamma}\right)H_k^{\Gamma i}T^{n+1}$$

contribute to the current stiffness matrix, that all others contribute only to the right-hand side, and that the right-hand side for the current step is calculated by adding terms to the right-hand side of the previous time increment.

4.4 *Procedures of analysis and sensitivity analysis*

Accounting for eqns (31) and (32), the discretized equations of momentum and energy can be written as:

$$\left(\frac{4m_{AB}\delta_{ik}}{\Delta t^2}+a_{BiAk}g_{n+1}^{G}+b_{BiAk}g_{n+1}^{\lambda}\right)u_k^{An+1}+c_{BiA}p_{n+1}^{K}T^{An+1}$$

$$= m_{AB}\left(\frac{4u_{in}^A}{\Delta t^2}+\frac{4\dot{u}_{in}^A}{\Delta t^2}+\ddot{u}_{in}^A\right)-a_{BiAk}f_n^{GAk}-b_{BiAk}f_n^{\lambda Ak}-c_{BiA}h_n^{KA}+G_{Bin+1} \tag{33}$$

$$\left(\frac{2d_{BAk}}{\Delta t}+f_{BAk}g_{n+1}^{\mathrm{d}K/\mathrm{d}t}\right)u_{kn+1}+\left(\frac{2g_{BA}}{\Delta t}+h_{BA}p_{n+1}^{\mathrm{d}m/\mathrm{d}t}+\kappa_{BA}\right)T^{An+1}$$

$$= d_{BAK}\left(\frac{2u_{kn}^A}{\Delta t}+\dot{u}_{kn}^A\right)-f_{BAk}f_n^{(\mathrm{d}K/\mathrm{d}t)Ak}+g_{BA}\left(\frac{2T_n^A}{\Delta t}+\dot{T}_n^A\right)-h_{BA}h_n^{\mathrm{d}m/\mathrm{d}t}+E_{n+1}^B \tag{34}$$

where superscripts G, λ, K, $\mathrm{d}K/\mathrm{d}t$, and $\mathrm{d}m/\mathrm{d}t$ denote kernels used in the calculations and f_n^Γ, g_{n+1}^Γ, h_n^Γ, and p_{n+1}^Γ are given by the following expressions for any kernel Γ:

$$f_n^\Gamma = \sum_{i=1}^{N} A_i^\Gamma \exp\left(-\frac{t_{n+1}}{v_i^\Gamma}\right)\sum_{k=0}^{n}(D_k^{\Gamma i}\dot{u}^k+F_k^{\Gamma i}u^k+G_{k-1}^{\Gamma i}u^k)$$

$$g_{n+1}^\Gamma = A_0^\Gamma+\sum_{i=1}^{N} A_i^\Gamma \exp\left(-\frac{t_{n+1}}{v_i^\Gamma}\right)G_n^{\Gamma i}$$

$$h_n^\Gamma = \sum_{i=1}^{N} A_i^\Gamma \exp\left(-\frac{t_{n+1}}{v_i^\Gamma}\right)\sum_{k=0}^{n}(H_{k-1}^{\Gamma i}-H_k^{\Gamma i})T^k$$

$$p_{n+1}^{\Gamma} = A_0^{\Gamma} + \sum_{i=1}^{\lambda} A_i^{\Gamma} \exp\left(-\frac{t_{n+1}}{v_i^{\Gamma}}\right) H_n^{\Gamma}.$$

Equations (33) and (34) contain the unknowns, the current displacements u_k^{An+1}, and temperatures T^{An+1}, which are premultiplied by partitions of the current stiffness matrix on the left-hand side, and the whole history of displacements and temperatures on the right-hand side.

Similarly, the DSA equations are obtained:

$$\left(\frac{4m_{AB}\delta_{ik}}{\Delta t^2} + a_{BiAk} g_{n+1}^{Ci} + h_{BiAk} g_{n+1}^{\prime i}\right)\frac{\mathrm{d}u_k^{An+1}}{\mathrm{d}b} + c_{BiA} p_{n+1}^{K} \frac{\mathrm{d}T^{An+1}}{\mathrm{d}b}$$

$$= -\frac{\partial\left(\frac{4m_{AB}\delta_{ik}}{\Delta t^2} + a_{BiAk} g_{n+1}^{Ci} + h_{BiAk} g_{n+1}^{\prime i}\right)}{\partial b} u_k^{An+1} - \frac{\partial c_{BiA} p_{n+1}^{K}}{\partial b} T^{An+1}$$

$$+ \frac{\partial m_{AB}}{\partial b}\left(\frac{4u_{in}^{A}}{\Delta t^2} + \frac{4\dot{u}_{in}^{A}}{\Delta t^2} + \ddot{u}_{in}^{A}\right) - \frac{\partial a_{BiAk}}{\partial b} f_n^{CiAk}$$

$$- \frac{\partial h_{BiAk}}{\partial b} f_n^{\prime iAk} - \frac{\partial c_{BiA}}{\partial b} h_n^{KA} + \frac{\partial G_{Bin+1}}{\partial b}$$

$$+ m_{AB}\left(\frac{4}{\Delta t^2}\frac{\mathrm{d}u_{in}^{A}}{\mathrm{d}b} + \frac{4}{\Delta t^2}\frac{\mathrm{d}\dot{u}_{in}^{A}}{\mathrm{d}b} + \frac{\mathrm{d}\ddot{u}_{in}^{A}}{\mathrm{d}b}\right) - a_{BiAk}\frac{\mathrm{d}f_n^{CiAk}}{\mathrm{d}b}$$

$$- h_{BiAk}\frac{\mathrm{d}f_n^{\prime iAk}}{\mathrm{d}b} - c_{BiA}\frac{\mathrm{d}h_n^{KA}}{\mathrm{d}b} \tag{35}$$

$$\left(\frac{2d_{BAk}}{\Delta t} + f_{BAk} g_{n+1}^{\mathrm{dK\,d}t}\right)\frac{\mathrm{d}u_{kn+1}}{\mathrm{d}b} + \left(\frac{2g_{BA}}{\Delta t} + h_{BA} p_{n+1}^{\mathrm{dm\,d}t} + \kappa_{BA}\right)\frac{\mathrm{d}T^{An+1}}{\mathrm{d}b}$$

$$= -\frac{\partial\left(\frac{2d_{BAk}}{\Delta t} + f_{BAk} g_{n+1}^{\mathrm{dK\,d}t}\right)}{\partial b} u_{kn+1} - \frac{\partial\left(\frac{2g_{BA}}{\Delta t} + h_{BA} p_{n+1}^{\mathrm{dm\,d}t} + \kappa_{BA}\right)}{\partial b} T^{An+1}$$

$$+ \frac{\partial d_{BAk}}{\partial b}\left(\frac{2u_{kn}^{A}}{\Delta t} + \dot{u}_{kn}^{A}\right) - \frac{\partial f_{BAk}}{\partial b} f_n^{\mathrm{dK\,d}t\,AK} + \frac{\partial g_{BA}}{\partial b}\left(\frac{2T_n^{A}}{\Delta t} + \dot{T}_n^{A}\right) - \frac{\partial h_{BA}}{\partial b} h_n^{\mathrm{dm/d}t}$$

$$+ d_{BAk}\left(\frac{2}{\Delta t}\frac{\mathrm{d}u_{kn}^{A}}{\mathrm{d}b} + \frac{\mathrm{d}\dot{u}_{kn}^{A}}{\mathrm{d}b}\right) - f_{BAk}\frac{\mathrm{d}f_n^{\mathrm{dK\,d}t\,AK}}{\mathrm{d}b} + g_{BA}\left(\frac{2}{\Delta t}\frac{\mathrm{d}T_n^{A}}{\mathrm{d}b} + \frac{\mathrm{d}\dot{T}_n^{A}}{\mathrm{d}b}\right)$$

$$- h_{BA}\frac{\mathrm{d}h_n^{\mathrm{dm\,d}t}}{\mathrm{d}b} + \frac{\mathrm{d}E_{n+1}^{B}}{\mathrm{d}b}. \tag{36}$$

Comparing eqns (33), (34) and (35), (36) one can see that the current stiffness matrices are the same for both analysis and DSA. It is also clear that the right-hand sides of both analysis and DSA are incremented from one time increment to the next. It is further observed that the right-hand side of the sensitivity equations depends on the whole history of sensitivities of displacements, velocities, and accelerations as well as displacements, velocities, and accelerations themselves. Hence, for sensitivity calculations, a DSA similar to the original FE analysis has to be carried along in every time step. An FE code based on the elements described above and capable of both analysis and DSA based on the above equations was developed. Partial derivatives, present on the right-hand side of the sensitivity

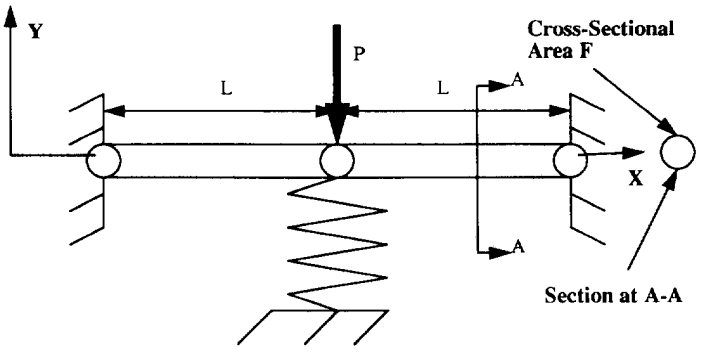

Fig. 1. Truss structure.

equations, were implemented via central differences, that is by utilizing the semi-analytical method. The central difference method provides ease and generality in coding, yet overcomes certain intrinsic inaccuracies of the semi-analytical method if forward differences are used. The errors in the semi-analytical method were first reported by Barthelemy and Haftka (1988), and then the rigid motion test was developed by Cheng and Olhoff (1993), in whose paper many other references on the subject can be found. Examples of its application are given in the next section. Analysis and DSA for non-linear trusses follow a similar route, but the current tangent stiffness matrix is used instead of the stiffness matrix.

5. NUMERICAL EXAMPLES

5.1 *Non-linear truss*

For verification of sensitivity analysis for trusses with large displacements, a model of truss shown in Fig. 1 was assembled. Material properties of the truss were assumed to be those of aluminum at elevated temperature and taken from Tauchert (1967). All units are in the SI system. The properties have the following values: $A_0^G = 2.65 \times 10^{10}$, $A_1^G = 2.34 \times 10^{10}$, $\nu^G = 0.88$, $A_0^K = 6.89 \times 10^{10}$, $A_1^K = 0.0$, $A_0^m = 1100.00$, $A_1^m = 0.0$, $\rho = 2702.00$, $\alpha = 1.30 \times 10^{-5}$, $\kappa = 225.00$. The initial temperature is taken as $T_0 = 733.00$ on the absolute scale. The external force P is harmonic as $P = A \sin t$ with the amplitude $A = 20{,}000.00$. The cross-sectional area F, length of bars L, and spring rate S were taken as follows: $F = 6.45 \times 10^{-6}$, $L = 0.40$, $S = 5.00$. Owing to the symmetry of the structure, only the left half of it with appropriate boundary conditions was analyzed. Figures 2 and 3 present histories of the midpoint displacement and temperature.

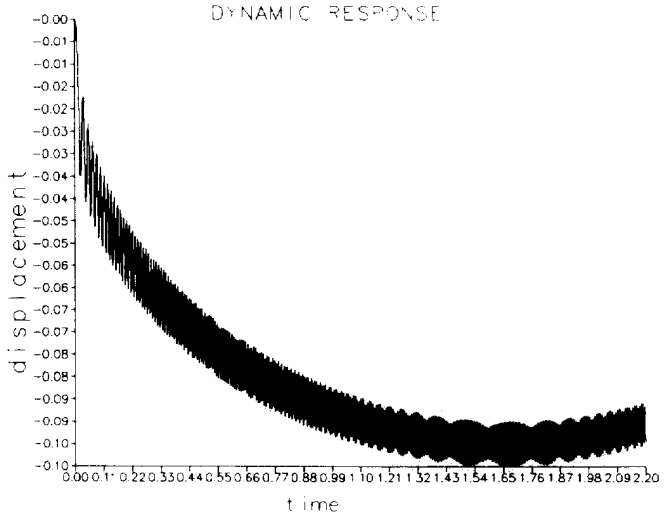

Fig. 2. Displacement history.

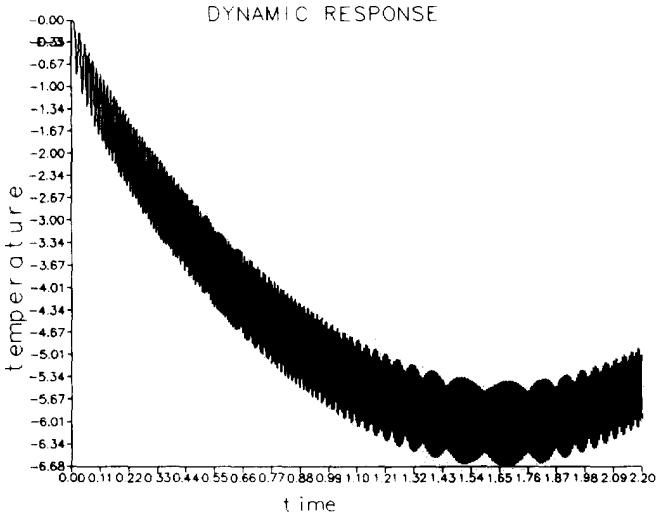

Fig. 3. Temperature history.

The same problem was modeled by using the IMSL Runge–Kutta subroutine for verification. Comparison of displacements and temperature at randomly selected times is presented in Tables 1 and 2.

It is clear from Tables 1 and 2 that there is a good agreement between the calculated response and one obtained by using the Runge–Kutta subroutine, which verifies the developed code.

Sensitivities of the calculated response with respect to the coefficient of thermal expansion were calculated and compared with the ones obtained by using the finite difference approach. Comparison of displacement sensitivities for several time instants is given in Table 3, and comparison of temperature sensitivities is given in Table 4.

Sensitivities calculated by using the developed approach and those obtained by finite differences practically coincide, and hence all differences in Tables 3 and 4 are zeros verifying the approach.

Table 1. Displacement comparison

Time (s)	Computed displacement (m)	Displacement by Runge–Kutta (m)	% Difference
0.12252	$-0.49828E-1$	$-0.49827E-1$	0.002
0.46024	$-0.77979E-1$	$-0.77985E-1$	0.008
0.83409	$-0.86345E-1$	$-0.86381E-1$	0.042
1.3006	$-0.93659E-1$	$-0.93590E-1$	0.074
1.9871	-0.10044	-0.10052	0.080

Table 2. Temperature comparison

Time (s)	Computed temperature (K)	Temperature by Runge–Kutta (K)	% Difference
0.12252	$-0.15588E-2$	$-0.15587E-2$	0.006
0.46024	$-0.38177E-2$	$-0.38182E-2$	0.013
0.83409	$-0.46807E-2$	$-0.46847E-2$	0.085
1.3006	$-0.55073E-2$	$-0.54992E-2$	0.147
1.9871	$-0.63338E-2$	$-0.63437E-2$	0.156

Table 3. Comparison of displacement sensitivity for truss

Time (s)	Calculated sensitivity	Finite difference	% Difference
0.36128E−2	0.88220E−1	0.88220E−1	0.0
0.11623E−1	0.17330	0.17330	0.0
0.40840E−1	−0.17687E−1	−0.17687E−1	0.0
0.87179E−1	0.14757E+1	0.14757E+1	0.0
0.14938	0.26354E+1	0.26354E+1	0.0

Table 4. Comparison of temperature sensitivity for truss

Time (s)	Calculated sensitivity	Finite difference	% Difference
0.36128E−2	−0.28797E+3	−0.28797E+3	0.0
0.11623E−1	−0.32545E+3	−0.32545E+3	0.0
0.40840E−1	−0.13137E+4	−0.13137E+4	0.0
0.87179E−1	−0.19178E+4	−0.19178E+4	0.0
0.14938	−0.26503E+4	−0.26503E+4	0.0

5.2 *2D Shape sensitivity analysis*

The program developed was used to analyze a 2D plane-strain problem. The structure under consideration is given in Fig. 4. It is a square plate with a hole in the center loaded with a uniformly distributed pressure P along the edges. The pressure varies harmonically with time as $P = A \sin t$, with the amplitude $A = 15$. The material properties of aluminum at the elevated temperature of 733 K, the same as in the case of the truss analysis of the previous section, are assumed here. A temperature equal to the initial temperature was prescribed along the edges of the hole. The outer edges of the plate carrying the load were insulated. Owing to the symmetry of the structure, only a quarter of it with the appropriate boundary conditions was analyzed; its FE mesh with node numbers is shown in Fig. 5. The time increment was taken as $\pi/20$, and analysis was carried out for 30 time steps. In this way, the structure goes through both tension and compression, since the external load changes its sign. The deformed plots of the structure after 10 and 30 time increments are shown in Figs 6 and 7, respectively, where the displacements are exaggerated in order to visualize the deformed configuration.

Shape sensitivity analysis with respect to the length of the center hole or the hole dimension in the X direction was performed by using the code developed. Both displacement and temperature sensitivities were calculated at every time step. Sensitivities were also

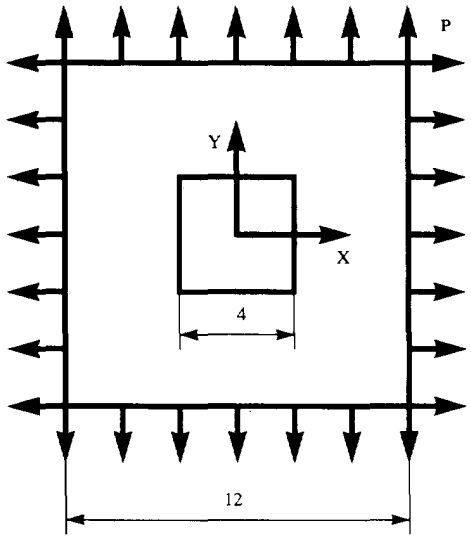

Fig. 4. Square plate with central hole under uniform pressure.

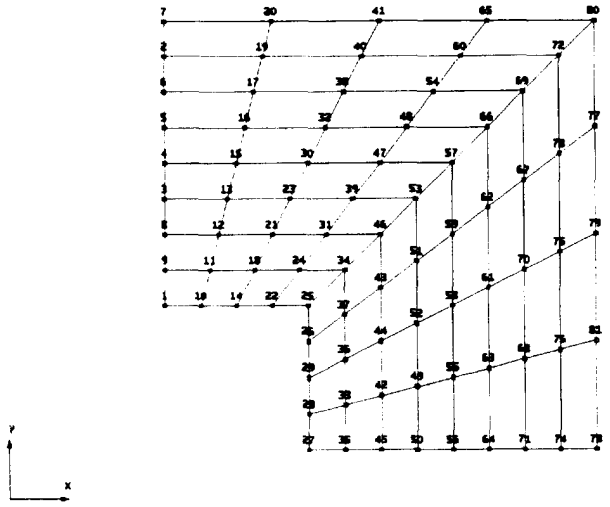

Fig. 5. Finite element mesh with node numbers.

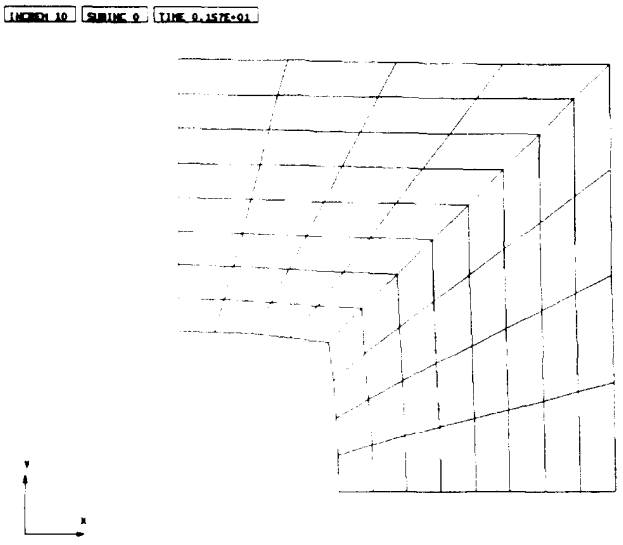

Fig. 6. Deformed plot after 10 time increments.

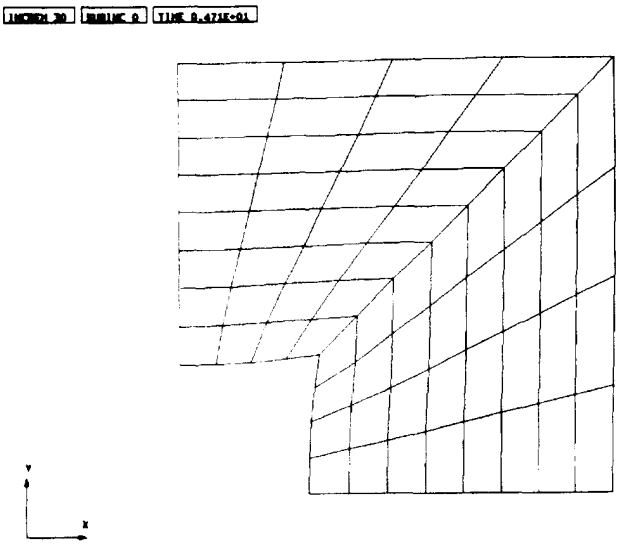

Fig. 7. Deformed plot after 30 time increments.

Table 5. Shape sensitivity analysis: comparison of displacement sensitivities

Time step	Node	Degreesof freedom	Calculated sensitivity	Finite difference	% Difference
10	18	1	0.12514E−2	0.12513E−2	0.01
10	18	2	−0.92703E−2	−0.92680E−2	0.02
10	49	1	0.58339E−3	0.58306E−3	0.06
10	49	2	−0.10569E−3	−0.10560E−3	0.09
10	53	1	−0.99835E−4	−0.99999E−4	0.05
10	53	2	−0.29350E−2	−0.29340E−2	0.03
30	18	1	−0.12064E−2	−0.12060E−2	0.03
30	18	2	0.83881E−2	0.83880E−2	0.0
30	49	1	−0.56606E−2	0.56600E−2	0.01
30	49	2	0.93544E−3	0.93600E−3	0.06
30	53	1	0.67500E−4	0.67558E−4	0.09
30	53	2	0.26571E−2	0.26560E−2	0.04

Table 6. Shape sensitivity analysis: comparison of temperature sensitivities

Time step	Node	Calculated sensitivity	Finite difference	% Difference
10	18	−0.14420E−2	−0.14420E−2	0.0
10	49	0.31992E−2	0.32000E−3	0.03
10	53	0.46890E−3	0.47000E−3	0.23
30	18	0.14891E−2	0.14900E−2	0.06
30	49	−0.31499E−3	0.31400E−3	0.32
30	53	−0.44950E−3	0.44800E−3	0.33

calculated by employing finite differences. The finite difference sensitivity results were used for comparison and verification of the approach developed and the code. Comparison of the finite difference sensitivities and those calculated by using the code developed is given in Tables 5 and 6. Table 5 presents comparison of displacement sensitivities and Table 6 presents comparison of the temperature sensitivities. Examination of the tables indicates that agreement between the calculated and finite difference sensitivities is quite good, which thus provides verification for the approach developed.

6. SUMMARY AND CONCLUSIONS

The equations of motion as well as the sensitivity equations for the direct differentiation method were transformed into a weak form and discretized by using the finite element method in the displacement form. In the temporal domain, the Newmark numerical scheme was used for discretization of the momentum equations, whereas the Crank–Nicholson scheme is used for discretization of the energy conservation equation. After the discretization, it was observed that, in the direct differentiation method, the discretized equations use the current tangent stiffness matrix. Use of the same discretization for both analysis and sensitivity analysis is emphasized. An FE code capable of analysis and DSA of 1D and 2D thermoviscoelastic problems was developed on the basis of the Christensen–Naghdi free energy function and the direct differentiation approach. A semi-analytical, central difference method was used in the implementation. The sensitivity results were verified via an overall central difference method.

The adjoint sensitivity equations derived by Poldneff and Arora (1993) can also be discretized by using the same procedures as described here for the direct differentiation method. The adjoint discretized sensitivity equations use the transpose of the current tangent stiffness matrix. Furthermore, the adjoint problem is a terminal value problem, which complicates its numerical implementation.

On the basis of the present study, the following conclusions can be drawn.

1. Sensitivity analysis of thermoviscoelastic structural systems is feasible and can be incorporated into a finite element computer code for dynamic response.

2. Very good accuracy in DSA of thermoviscoelastic structural systems can be achieved.
3. The direct differentiation method is better suited for computer implementation of thermoviscoelastic systems as compared with the adjoint variable method because it is an initial value problem and can march in time together with the original analysis problem. The adjoint variable method results in a terminal value problem, and the sensitivity analysis can therefore be performed only after the analysis is completed.
4. Implementation of DSA depends on the thermoviscoelastic constitutive law and its implementation since the sensitivity distribution depends on the whole history of response and sensitivities.

Acknowledgement—The authors are grateful to The Goodyear Tire & Rubber Company for support and permission to publish their results.

REFERENCES

Barthelemy, B. and Haftka, P. M. (1988). Accuracy analysis of semi-analytical method for shape sensitivity calculation. In *AIAA/ASME/ASCE/AHS/ASC, 29th Structures, Structural Dynamics and Materials Conference*, Williamsburg, Virginia, USA, 18–20 April, pp. 572–581.

Cheng, G. and Olhoff, N. (1993). Rigid body motion test against error in semi-analytical sensitivity analysis. *Comput. Struct.* **46,** 515–527.

Christensen, R. M. and Naghdi, P. M. (1967). Linear non-isothermal viscoelastic solids. *Acta Mech.* **3,** 1–12.

Dems, K. (1987). Sensitivity analysis in thermoelasticity problems. In *Computer Aided Optimal Design: Structural and Mechanical Systems* (Edited by C. A. Mota Soares) (NATO ASI Series). **F27,** pp. 563–572. Springer-Verlag, Berlin and Heidelberg, Germany.

Dems, K. and Mroz, Z. (1987). Variational approach to sensitivity analysis in thermoelasticity. *J. Therm. Stresses* **10,** 283–306.

Hou, G. J. W., Sheen, J. S. and Chuang, C. H. (1990). Shape sensitivity analysis and design optimization of linear, thermoelastic solids. In *AIAA/ASME/ASCE/AHS/ASC, 31st Structures, Structural Dynamics and Materials Conference*, Long Beach, California, USA, 2–4 April, pp. 206–216.

Jao, S. Y. and Arora, J. S. (1992). Design sensitivity analysis of nonlinear structures using endochronic constitutive model. Part 2: Discretization and applications. *Comput. Mech.* **10,** 59–72.

Lee, T. H., Arora, J. S. and Rim, K. (1991). Design sensitivity analysis of thermoviscoplastic mechanical and structural systems. *Technical Report No.ODL-91.19*. Optimal Design Laboratory, College of Engineering, University of Iowa, Iowa City, IA, USA.

Lee, T. H., Arora, J. S. and Kumar, V. (1993). Shape design sensitivity analysis of viscoplastic mechanical structures. *Comp. Meth. Appl. Mech. Engng* **108,** 237–259.

Meric, R. A. (1986a). Material and load optimization of thermoelastic solids. Part I: Sensitivity analysis. *J. Therm. Stresses* **9,** 359–372.

Meric, R. A. (1986b). Material and load optimization of thermoelastic solids. Part II: Numerical results. *J. Therm. Stresses* **9,** 373–388.

Meric, R. A. (1987). Sensitivity analysis for a general performance criterion in micropolar thermoelasticity. *Int. J. Engng Sci.* **25,** 265–276.

Meric, R. A. (1988). Sensitivity analysis of functionals with respect to shape for dynamically loaded nonlocal thermoelastic solids. *Int. J. Engng Sci.* **26,** 703–711.

Meric, R. A. (1990). Simultaneous material load shape variations of thermoelastic structures. *AIAA J.* **28,** 296–302.

Oden, J. T. (1972). *Finite Elements of Nonlinear Continua* McGraw-Hill, New York, NY, USA.

Poldneff, M. J. & Arora, J. S. (1993). Design sensitivity analysis of coupled thermoviscoelastic systems. *Int. J. Solids & Structures* **30,** 607–635.

Tauchert, T. R. (1967). Heat generation in a viscoelastic solid. *Acta Mech.* **3,** 385–396.

Tortorelli, D. A., Haber, R. A. and Lu, S. C.-Y. (1991). Adjoint sensitivity analysis of nonlinear dynamic thermoelastic systems. *AIAA J.* **29,** 296–302.

Tortorelli, D. A., Subramani, G., Lu, S. C. Y. and Haber, R. B. (1991). Sensitivity analysis for Coupled thermoelastic systems. *Int. J. Solids Structures* **27,** 1477–1497.